

2D backward-mode photoacoustic imaging system for NIR (650-1200nm) spectroscopic biomedical applications

Edward Z. Zhang* and Paul Beard

Department of Medical Physics and Bioengineering, University College London
Malet Place Engineering Building, Gower Street, London WC1E 6BT, UK

ABSTRACT

A 2D photoacoustic imaging system for spectroscopic biomedical applications is reported, based on a Fabry-Perot (FP) polymer film ultrasound sensor. A variety of broadband sensors have been developed with bandwidths from 20MHz to 50MHz. These ultrasound sensors have a unique dichroic design which has an optical transmission window from 650nm to 1200nm and can be interrogated in the 1520-1610nm wavelength region. This enables the system to operate in backward mode with a tunable Optical Parametric Oscillator (OPO) as the excitation source for near infrared (NIR) spectroscopic applications such as the measurement of blood oxygenation. The area over which the photoacoustic signals can be mapped is 4cm × 2.5cm with an optically defined element size of 64μm diameter. The system's noise-equivalent pressure (NEP) is 0.3kPa over a 20MHz bandwidth without signal averaging. The photoacoustic signals are mapped by rapidly scanning a focused laser beam over the surface of the sensor with a point to point acquisition time of 100ms. The spatial resolution of the imaging system, evaluated from tests on phantoms using a 50MHz FP sensor, is 37μm (lateral) × 27μm (vertical) FWHM. It is considered that this system has the potential to be used in applications that require high resolution 3D imaging of the structure and oxygenation status of the microvasculature.

Keywords: Photoacoustic, ultrasound array, biomedical, imaging, Fabry Perot sensor, 2D scanning

1. INTRODUCTION

Photoacoustic imaging offers an effective tool for imaging soft tissue. It relies upon the generation of acoustic energy inside a volume of tissue by illuminating it with pulsed visible or NIR laser light. Broadband (tens of MHz) pulses of acoustic energy, emitted by preferentially optically absorbing subsurface anatomical structures such as blood vessels, propagate to the surface where they are detected by an array of ultrasound receivers. By measuring the time of arrival of the acoustic pulses at each element of the array, and with knowledge of the speed of sound in tissue, the acoustic signals can be spatially resolved and backprojected to form an image of the internally distributed photoacoustic sources. By encoding the spatial distribution of tissue optical properties on to broadband ultrasound waves in this way, the technique combines the advantages of the strong contrast and spectroscopic capability offered by optical methods with the high spatial resolution available to ultrasound. Applications include imaging the breast for the diagnosis and screening of cancer [1, 2], the assessment of vascular disease [3], structural and functional imaging of the brain [4] and imaging the microvasculature [5, 6, 7].

For short range high resolution applications, such as imaging the skin where it is required to visualise microvessels that lie within a few mm of the surface, it is highly desirable to be able to detect the photoacoustic signals over the same region of the tissue surface that is irradiated: the so-called backward mode of operation. In this paper we report a 2D photoacoustic imaging system based on a Fabry-Perot (FP) polymer film ultrasound sensor [8,9,10,11,12] that can achieve this. In contrast to a previously described FP sensor, which was designed to be transparent to excitation laser pulses at 1064nm [13], the sensor is transparent in the wavelength range 650nm-1200nm and thus coincides with the so-called NIR window of transparency for biological tissues. This enables the system to operate in backward mode with a tunable Optical Parametric Oscillator (OPO) as the excitation source for near infrared (NIR) spectroscopic applications such as the measurement of blood oxygenation [14,15]. In section 2, the design of the FP polymer film ultrasound sensor and the experimental setup of the photoacoustic imaging system are described. The image resolution of the system in terms of its point spread function (PSF), and acoustic detection sensitivity are discussed in section 3. The

* ezhang@medphys.ucl.ac.uk; phone +44 20 7679 0281

system has been demonstrated by using it to obtain 3D images of a range of dye and blood filled tubes immersed in Intralipid as described in section 4.

2. EXPERIMENTAL SETUP

A schematic of the 2D photoacoustic imaging system is depicted in Figure 1(a). The excitation source is an optical fiber coupled tunable OPO laser (630–1200nm) or a Q-switched pulsed Nd:YAG laser operating at 1064nm. The structure of the FP sensor is illustrated in Figure 1(b). It is of lateral dimensions of 25mm×40mm and comprises a Fabry-Perot (FP) polymer film interferometer, which consists of a Parylene film with dielectric coatings at its two facets [10]. The sensing structure (including the Parylene film) is vacuum deposited on to a polymer substrate [10]. The thickness of the film is either of 20μm or 40μm, giving rise to an acoustic bandwidth of 25 or 50MHz respectively. The dielectric coatings have a dichroic design, the spectral transmission characteristics of which are shown in Figure 1(c), and have high reflectivity (>90%) in 1550nm band, while the excitation laser pulse in NIR region 650-1200nm can pass through it (>80% transmission).

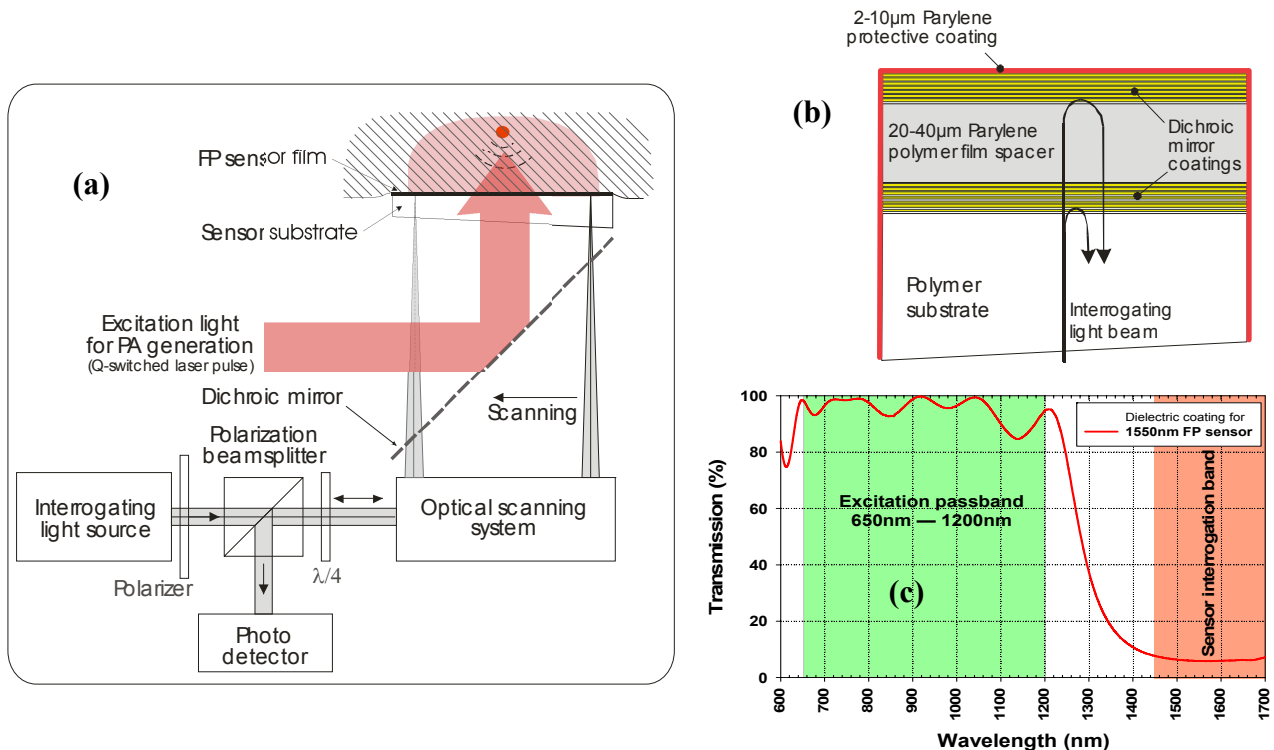


Figure 1: (a) Schematic of the backward mode 2D photoacoustic imaging system; (b) Configuration of the FP sensor; (c) Transmission characteristics of FPI dichroic mirrors.

The interrogating light source is a single mode wavelength tunable laser with a tuning range of 1519–1630nm, optical output power output of approximately 10mW, spectral line width (FWHM) <150 kHz and relative intensity noise (RIN) <140dB/Hz. The interrogating light is focused at and scanned across the FP sensor film using a 2D galvanometer-based optical scanning system. The scanning system and associated optics are also arranged to guide the interrogating light reflected from the FP sensor to an InGaAs photodiode (PD). The acoustic waveform detected by the PD is digitized by a digital oscilloscope and uploaded to a PC. At each scanning step, the wavelength of the interrogating light is tuned to the optimum phase bias point where the acoustic sensitivity is maximized, prior to the capture of each acoustic

waveform. The spot size of the interrogating light focused at the FP sensing element is $\sim 64\mu\text{m}$ diameter, which represents (to a first approximation) the active area of the sensor.

3. SYSTEM EVALUATION

To evaluate the PSF of the system, a phantom comprising 6 layers of parallel black polymer ribbons was constructed, as illustrated on the left of Figure 2. The widths of those black polymer ribbons in the lower 5 layers are $80\text{--}120\mu\text{m}$, and those for the top layer are $\sim 300\mu\text{m}$. The target was submerged in 1.5% Intralipid ($\mu_s' = 1\text{mm}^{-1}$) with all layers of the polymer ribbons parallel to the lateral plane of the FP sensor. The excitation was provided by the dual-wavelength outputs (637 and 800nm) from an OPO laser with a pulse duration of 8ns, repetition rate of 10Hz and beam diameter of 4cm. The total incident fluence was around $3.2\text{mJ}/\text{cm}^2$.

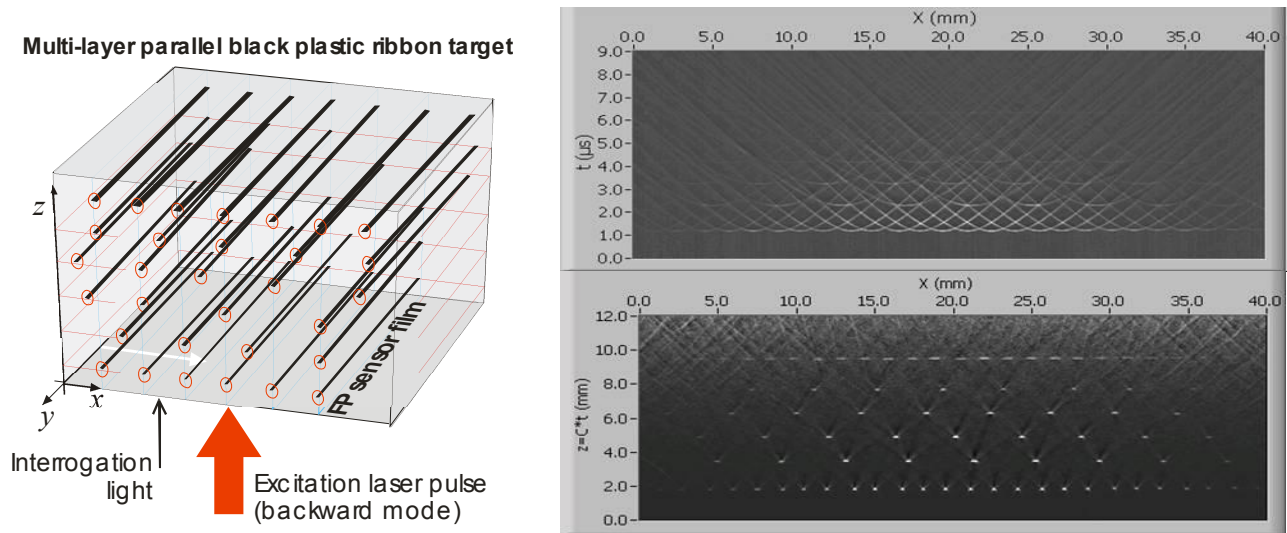


Figure 2: Cross sectional imaging of a target of multiple layers of black polymer ribbons for PSF assessment.

Using a $40\mu\text{m}$ thick FP polymer film sensor, a line scan was performed along the direction transverse to those ribbons depicted on the left of Figure 2, over a length of 40mm in steps of $20\mu\text{m}$. No signal averaging was used for these measurements. The mapped 2D (lateral x vs temporal z) acoustic field is presented in the grey-scaled intensity graph on top right corner of Figure 2. Beneath it is the cross-sectional image of the multi-layer ribbon target reconstructed from the mapped acoustic field using a k-space reconstruction algorithm [16]. The lateral PSF obtained from the reconstructed image shown in, is illustrated in Figure 3, where the PSF is defined as the full width at half maximum (FWFM) of the derivative of the edge spread function (ESF) of each reconstructed ribbon feature.

With this $40\mu\text{m}$ thick FP sensor and excitation pulse duration of 8ns, the minimum lateral PSF is $62\mu\text{m}$ as indicated in Figure 3. The vertical PSF is $50\mu\text{m}$. The lateral PSF remains less than $125\mu\text{m}$ for depths up to 9mm at the centre of the sensor, and over a lateral span of 40mm at 2mm depth. The PSF of this imaging system based on the $40\mu\text{m}$ thick sensor of 25MHz acoustic bandwidth, can be improved by using shorter excitation pulse durations (5.6ns instead of 8ns). The PSF can be further improved by using a $20\mu\text{m}$ thick FP sensor which provides a 50MHz acoustic bandwidth. The PSFs of the imaging system based on both $40\mu\text{m}$ and $20\mu\text{m}$ thick sensors are summarized in Table 1. The acoustic sensitivity of the system is approximately 0.3kPa NEP over a measurement bandwidth of 20MHz and without signal averaging.

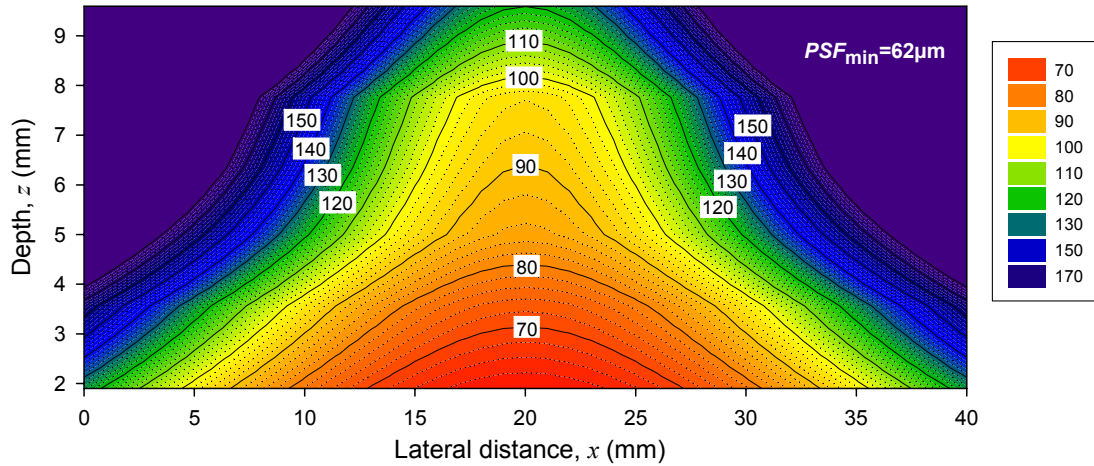


Figure 3: Lateral point spread function (PSF) for a 40µm thick FP polymer film sensor.

Table 1: PSF vs sensor film thickness and excitation pulse duration

Sensor film thickness	Vertical <i>PSF</i>		Lateral <i>PSF</i> _{min}	
	(Δt) _{ex} =8ns	(Δt) _{ex} =5.6ns	(Δt) _{ex} =8ns	(Δt) _{ex} =5.6ns
40µm	50µm	34.2µm	62µm	52µm
20µm	36µm	27µm	47µm	37µm

4. 3D IMAGING OF PHANTOMS

The 2D photoacoustic imaging system was used in backward mode to map the acoustic fields generated in various absorptive objects submerged in 1.5% Intralipid and illuminated by a Q-switched Nd:YAG pulse laser operating at 1064nm and a 20Hz repetition rate. The incident fluence was $\sim 15\text{mJ}/\text{cm}^2$. The distance of these objects from the sensor plane ranged from 1mm to 5mm. The photoacoustic signals were mapped (without signal averaging) by scanning the sensor interrogating beam in 2D dimensions. 3D images were then reconstructed from the detected time resolved photoacoustic signals [17] and maximum intensity (MI) projections formed from these. Figure 4 shows the photograph of one of the absorptive objects imaged, a knotted 300µm bore silicone rubber tube filled with NIR dye ($\mu_a > 10\text{mm}^{-1}$) and the MI projections on to the lateral and vertical planes. The lateral maximum intensity (MI) projections obtained from the 3D photoacoustic images of the other absorptive objects imaged are shown in Figure 5.

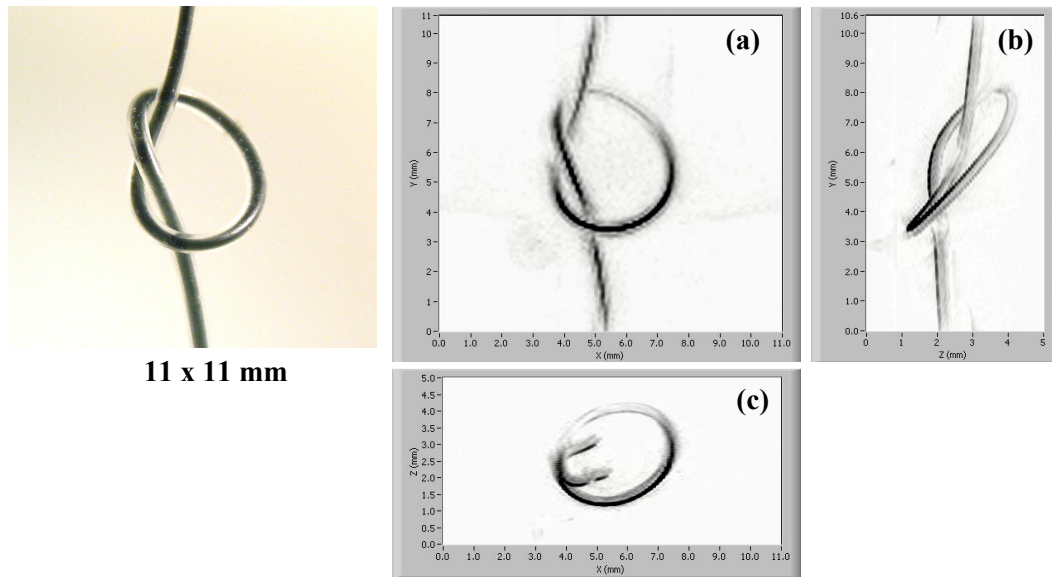


Figure 4: Photograph (upper left) of a knotted 300 μ m bore silicone rubber tube filled with absorbing NIR dye. The tube was immersed in a solution of 1.5% Intralipid ($\mu_s'=1\text{mm}^{-1}$) at a distance of 2.5mm from the sensor plane. The MI projections obtained from the reconstructed 3D photoacoustic image are shown on the right: (a) lateral (x-y) plane, (b) vertical (x-z) plane, (c) vertical (z-y) plane

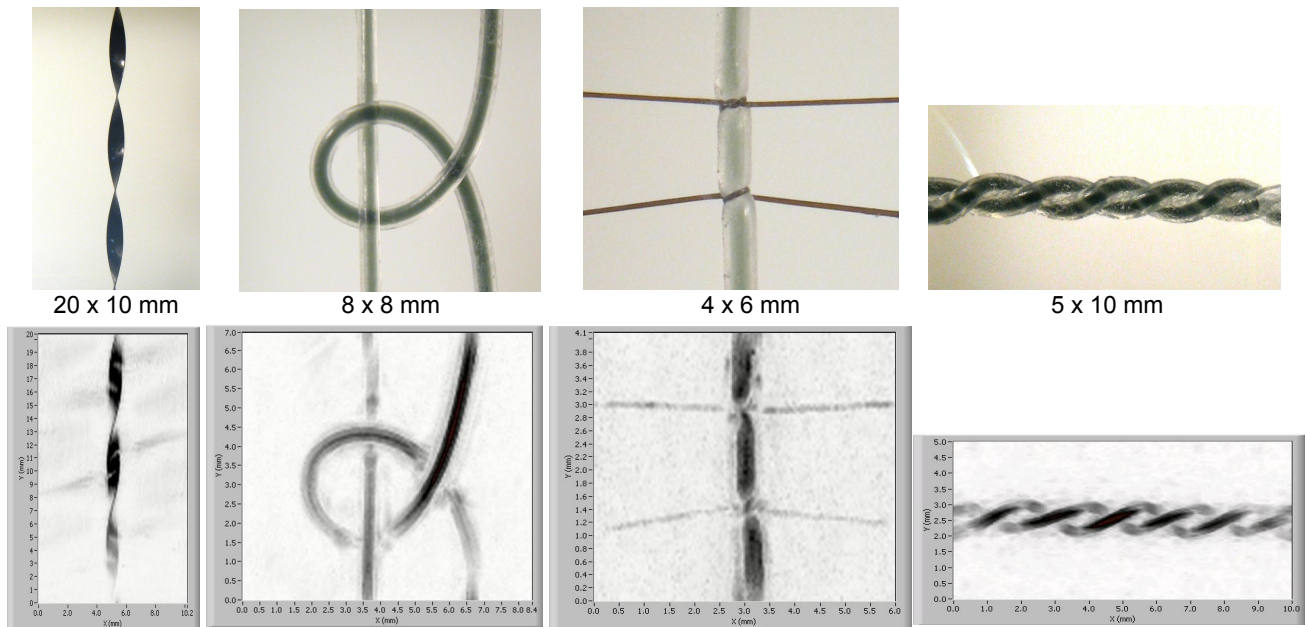


Figure 5: Upper row: photographs of absorptive objects imaged. From left to right: 1. twisted black polymer ribbon; 2. 300 μ m bore silicone rubber tubes filled with NIR dye ($\mu_a=2.7$ and 4mm^{-1} , respectively); 3. 300 μ m bore silicone rubber tube filled with NIR dye ($\mu_a=2.7\text{mm}^{-1}$) and tied with human hair; 4. Twisted pair of 300 μ m bore silicone rubber tubes filled with NIR dye ($\mu_a=2.7\text{mm}^{-1}$). Lower row: The Lateral MI projections obtained from the reconstructed 3D photoacoustic images of these objects.

In order to demonstrate the ability of the system to image the microvasculature, a network of tubes of inner diameters 64, 100 and 300 μm were filled with human blood (15.2g/dL hemoglobin) as shown in the photograph in Figure 6 on the left, and submerged in 1.5% Intralipid ($\mu_s' = 1\text{mm}^{-1}$). The 800nm output from the OPO laser operating at a repetition rate of 10Hz was used as the excitation source. The PA signals were mapped over a 100×100 element grid over an area of $14\text{mm} \times 14\text{mm}$ without signal averaging. The lateral MI projection of the reconstructed 3D image over a depth range from 0.5mm to 5.5mm, is displayed on the right of Figure 6. All tubes shown in the photograph on the left of Figure 6 can be clearly identified, except the central 300 μm tube which was around 10mm away from the FP sensor.

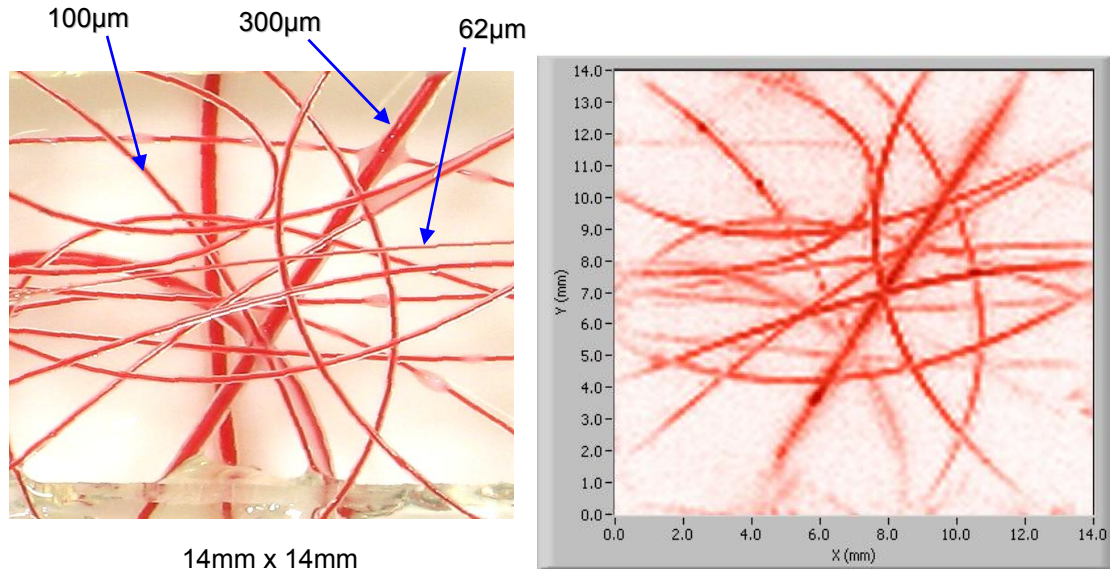


Figure 6: Human blood filled tubes (left) and the lateral MI projection (right) of their 3D photoacoustic image obtained in backward mode with 800nm excitation light pulses when submerged in 1.5% Intralipid ($\mu_s' = 1\text{mm}^{-1}$). Incident fluence: $6.7\text{mJ}/\text{cm}^2$

Figure 7 displays the lateral MI projections of the reconstructed 3D image of those blood-filled tubes shown in Figure 6 at different depth ranges. As shown in the figure, the 62 μm bore tube indicated in Figure 6 was located at depth between $z = 0.9\text{mm}$ and 1.1mm . Most of the 100 μm bore tubes were at $z = 1.1 - 3.5\text{mm}$. Two 300 μm and a few 100 μm bore tubes were at $z = 3.5 - 5.5\text{mm}$.

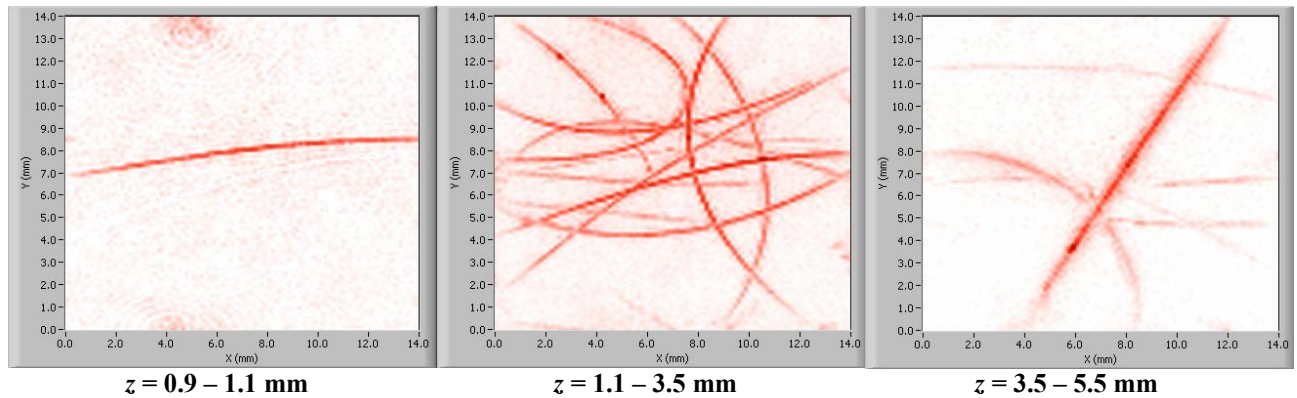


Figure 7: Lateral MI projections of the 3D photoacoustic image of the blood-filled tubes shown in Figure 6 at various depth ranges.

5. CONCLUSION

The feasibility of using the Fabry Perot polymer film ultrasound sensing concept for short range (<1cm), high resolution backward mode photoacoustic imaging has been demonstrated. By imaging a physiologically realistic microvessel phantom, it has been shown that this type of instrument may be suitable for high resolution 3D imaging of the structure and function of superficial blood vessels such as those in the skin or superficial tumours.

ACKNOWLEDGEMENT

This work is sponsored by the Engineering and Physical Science Research Council, UK.

REFERENCES

1. Andreev VG, Karabutov AA, Solomatin SV, Savateeva EV, Aleynikov V, Zhulina YV, Fleming RD, Oraevsky AA, Photoacoustic tomography of breast cancer with arc-array-transducer, *Proc SPIE Vol 3916*, pp36-47, 2000
2. Kruger R.A., Miller K.D., Reynolds H.E., Kiser Jr W.L., Reinecke D.R. and Kruger G.A., Contrast enhancement of breast cancer in vivo using thermoacoustic CT at 434 MHz, *Radiology*, 216, pp.279-283, 2000
3. Beard PC and Mills TN, Characterisation of *post mortem* arterial tissue using time-resolved photoacoustic spectroscopy at 436nm, 461nm and 532nm, *Physics in Medicine and Biology*, Vol 42, No 1, pp177-198, 1997.
4. Wang X, Pang Y, Ku G, Xie X, Stoica G and Wang L, "Noninvasive laser-induced photoacoustic tomography for structural and functional *in vivo* image of the brain," *Nature Biotechnology*, 21 (7), pp.803-806 (2003).
5. Beard PC, Photoacoustic imaging of blood vessel equivalent phantoms, *Proc. SPIE*, Vol. 4618, pp.54-62, 2002.
6. Magdalena C. Pilatou, Nico J. Voogd, Frits F. M. de Mul, Wiendelt Steenberg, and Leon N. A. van Adrichem, Analysis of three-dimensional photoacoustic imaging of a vascular tree in vitro, *Rev. Sci. Instrum.* 74, pp.4495-4499, 2003.
7. Hoelen CG, de Mul FFM, Pongers R, Dekker A, Three-dimensional photoacoustic imaging of blood vessels in tissue, *Optics Letters*, Vol 23, No 8, pp648-650, 1998
8. Beard PC and Mills TN., An optical fibre sensor for the detection of laser generated ultrasound in arterial tissues, *Proc SPIE Vol 2331*, pp112-122, 1994
9. Beard PC, Perennes F, Mills TN, Transduction mechanisms of the Fabry Perot polymer film sensing concept for wideband ultrasound detection., *IEEE Transactions on Ultrasonics, Ferroelectrics and Frequency control*, Vol 46, No 6, pp1575-1582, 1999.
10. Zhang E. and Beard PC, Broadband ultrasound field mapping system using a wavelength tuned, optically scanned focussed beam to interrogate a Fabry Perot polymer film sensor, *IEEE Transactions on Ultrasonics, Ferroelectrics and Frequency control*, in press.
11. Lamont M and Beard PC, 2D imaging of ultrasound fields using a CCD array to detect the output of a Fabry Perot polymer film sensor, *Electronics Letters*, in press.
12. Askenazi S, Witte R, O'Donnell M, High frequency ultrasound imaging using a Fabry Perot etalon, *Proc SPIE Vol 5697*, pp243-250, 2005
13. Beard PC, Zhang EZ, Cox BT, Transparent Fabry Perot polymer film ultrasound array for backward-mode photoacoustic imaging, *Proc. SPIE 5320*, pp230-237, 2004
14. Laufer J, Elwell CE, Delpy DT, Beard PC, *In vitro* measurements of absolute blood oxygen saturation using pulsed near-infrared photoacoustic spectroscopy: accuracy and resolution, *Physics in Medicine and Biology*, 50, pp 4409–4428, 2005

- 15 Laufer J, Elwell C, Delpy D, Beard PC, Spatially resolved blood oxygenation measurements using time-resolved photoacoustic spectroscopy, *Oxygen Transport to Tissue XXVII*, Series: *Advances in Experimental Medicine and Biology*, Vol. 578, 155-160, 2006
16. K P Köstli and Paul C Beard, Two-dimensional photoacoustic imaging by use of Fourier-transform image reconstruction and a detector with an anisotropic response, *Applied Optics*, Volume 42, Issue 10, pp.1899-1908.
17. Koestli K, Frenz M, Bebie H, Weber H, Temporal backward projection of optoacoustic pressure transients using Fourier transform methods, *Physics in Medicine and Biology*, **46**, pp1863-1872, 2001